Electronic Supplementary Material (ESI) for Journal of Materials Chemistry

Supplemental information

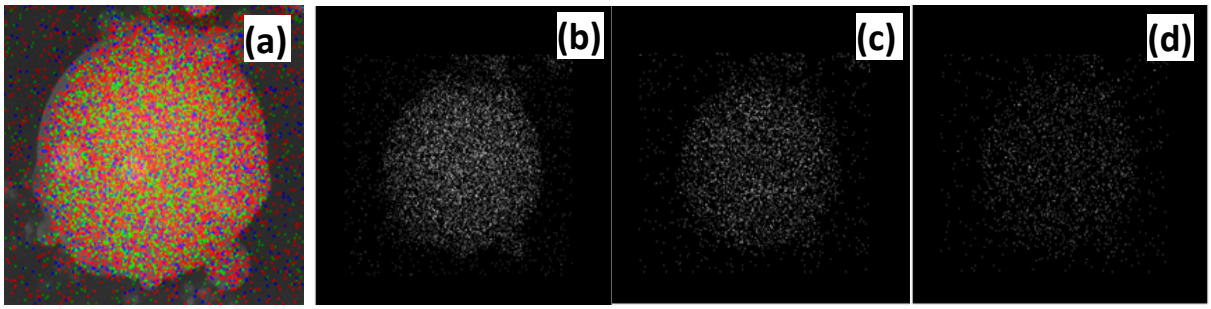

Figure S1A: element analysis of $TiO_2/SiO_2/Fe_2O_3$ precursor porous particles calcined at 500℃, (a) the red, green and blue spots represents Si, Ti and Fe respectively, (b) Si, (c) Ti, (d) Fe.

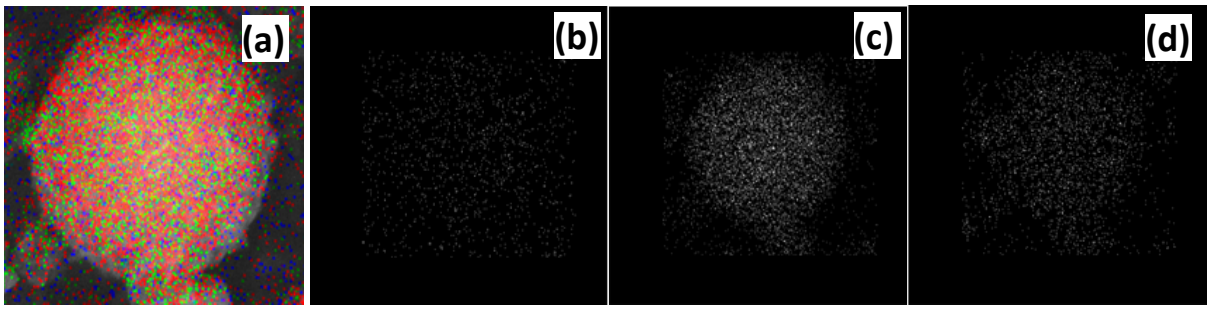

Figure S1B: element analysis of hollow TiO_2-SiO_2 spheres (etched from Figure S1A precursors), (a) the red, green and blue spots represents Ti, Fe and Si respectively, (b) Si, (c) Ti, (d) Fe.

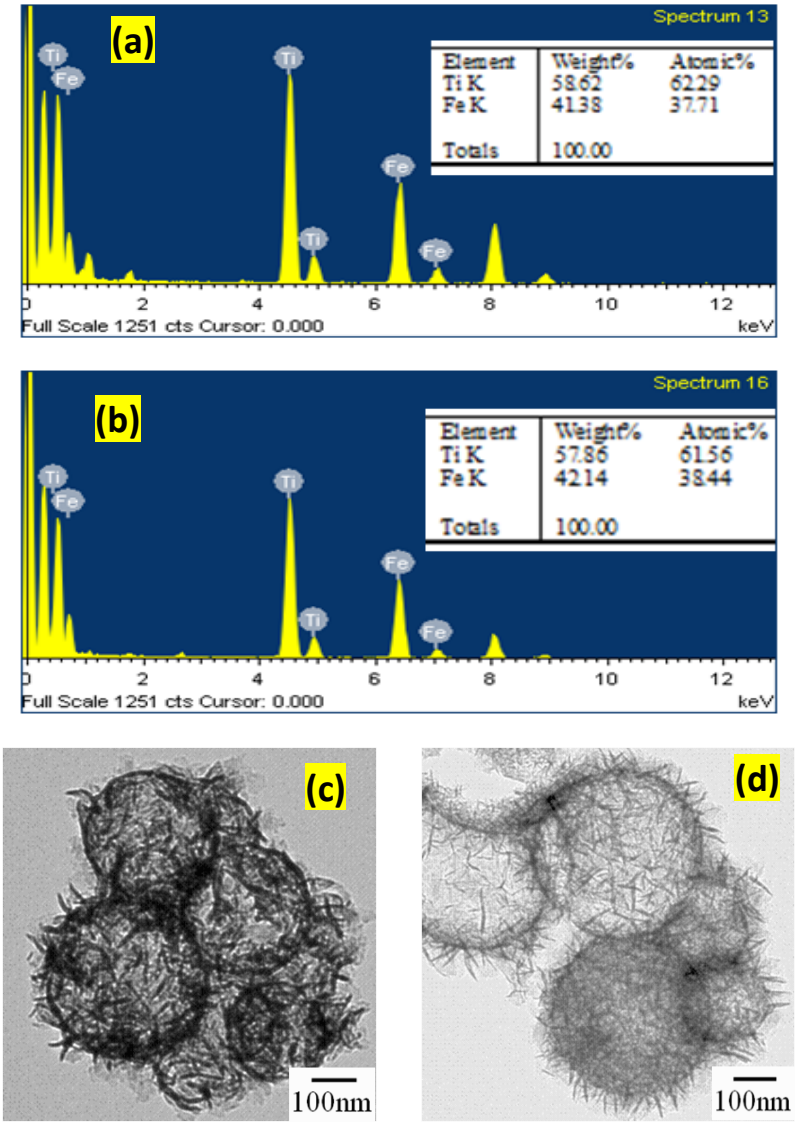

Figure S2 (a) The EDS spectrum of the nanofibers on hollow spheres, (b) nanofibers for the hollow spheres etched further using 0.1 M HCl solution for 3h. (c) TEM image of hollow spheres obtained by etching aerosol particles calcined at 500℃, (d) TEM image of the hollow particles etched further using 0.1 M HCl solution for 3h.

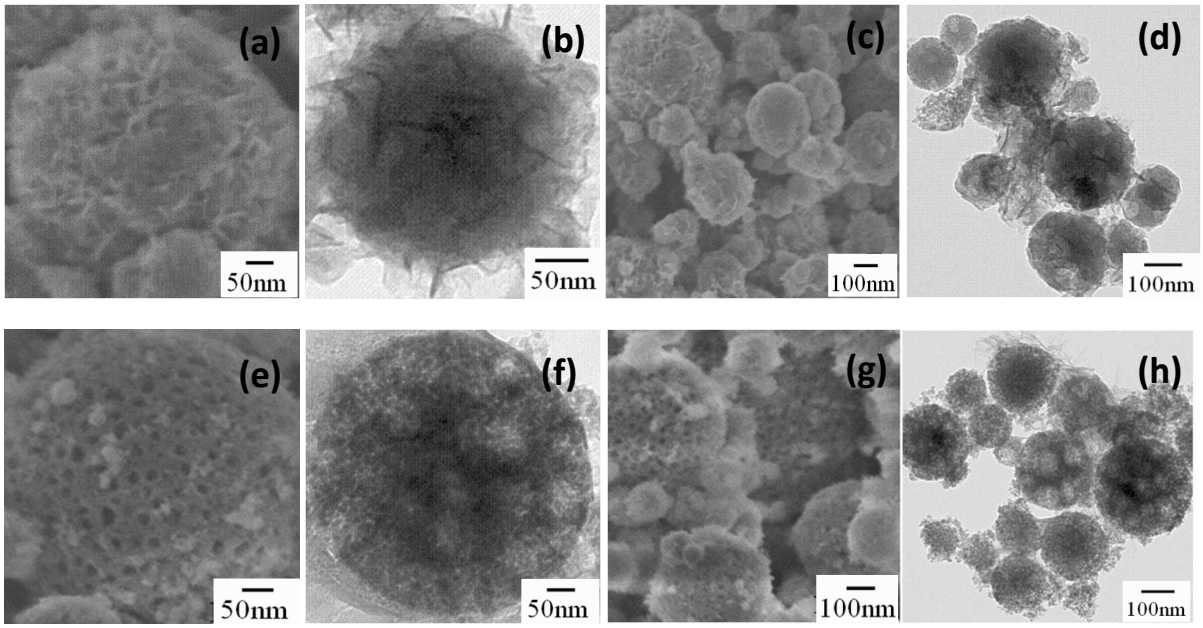

Figure S3 SEM and TEM images of spheres obtained by etching particles calcined at different temperatures, (a) (b) (c) (d) 700 ℃, (e) (f) (g) (h) 900 ℃.

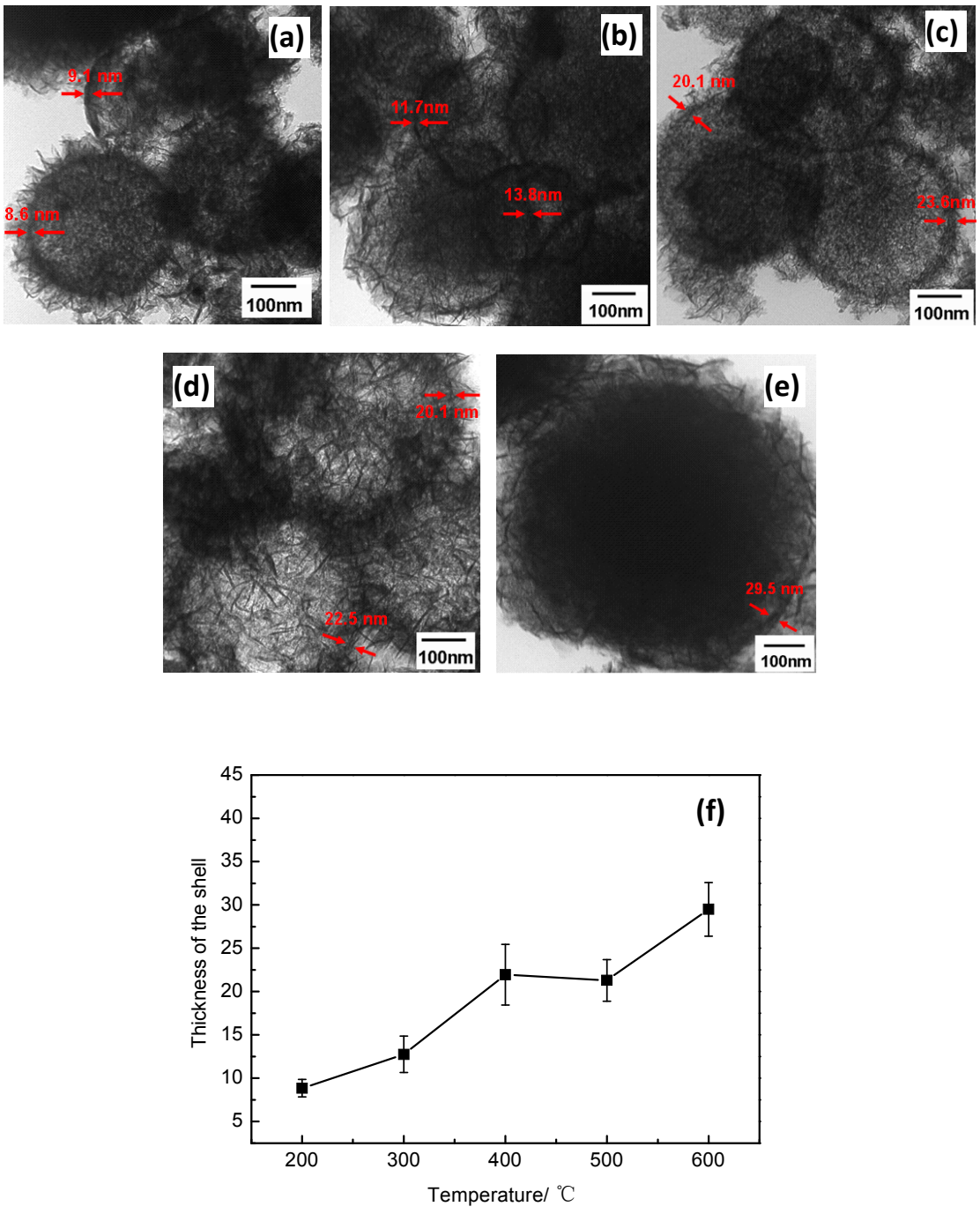

Figure S4: effect of temperature on the thickness of the shell of hollow spheres, (a) 200℃, (b) 300℃, (c) 400℃, (d) 500℃, (e) 600℃, (f) the thickness of the shell increase with increasing the calcination temperature of the precursor particles. (5 wt% NaOH solution, 3h)

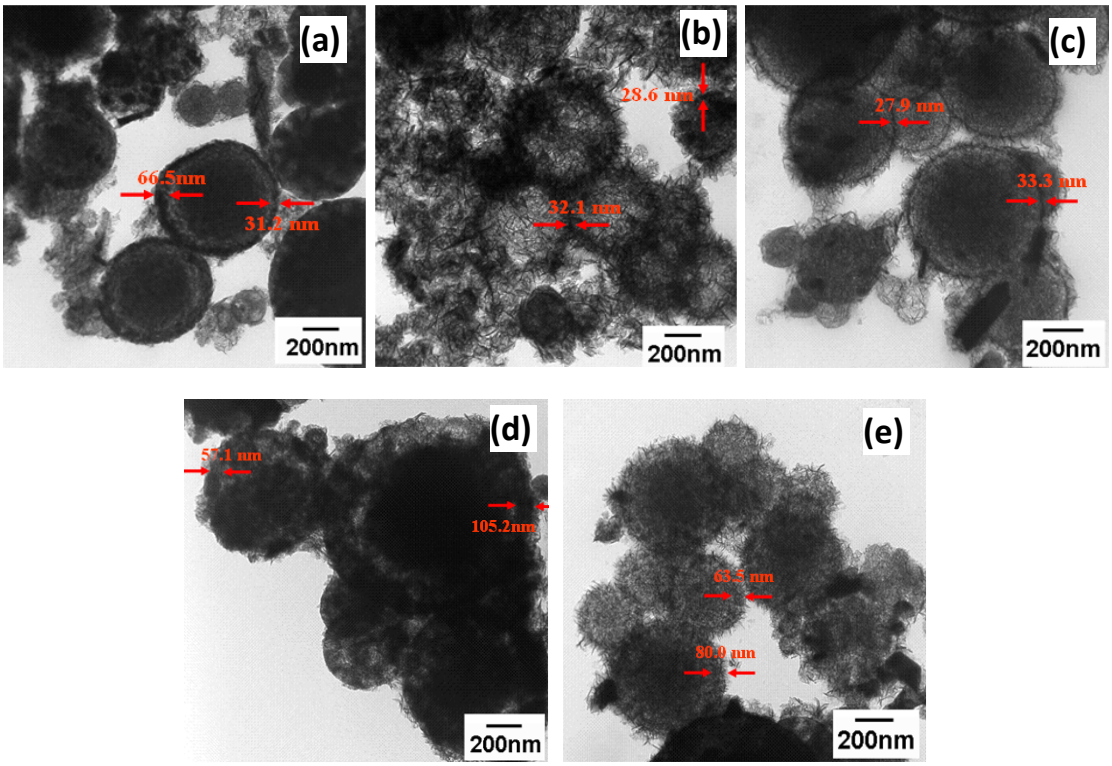

Figure S5: effect of the calcination time of the precursor particles on the structures of etched spheres, (a) 1h, (b) 3h, (c) 5h, (d) 7h, (e) 9h. Etching conditions: 5wt% NaOH solution for 3h.

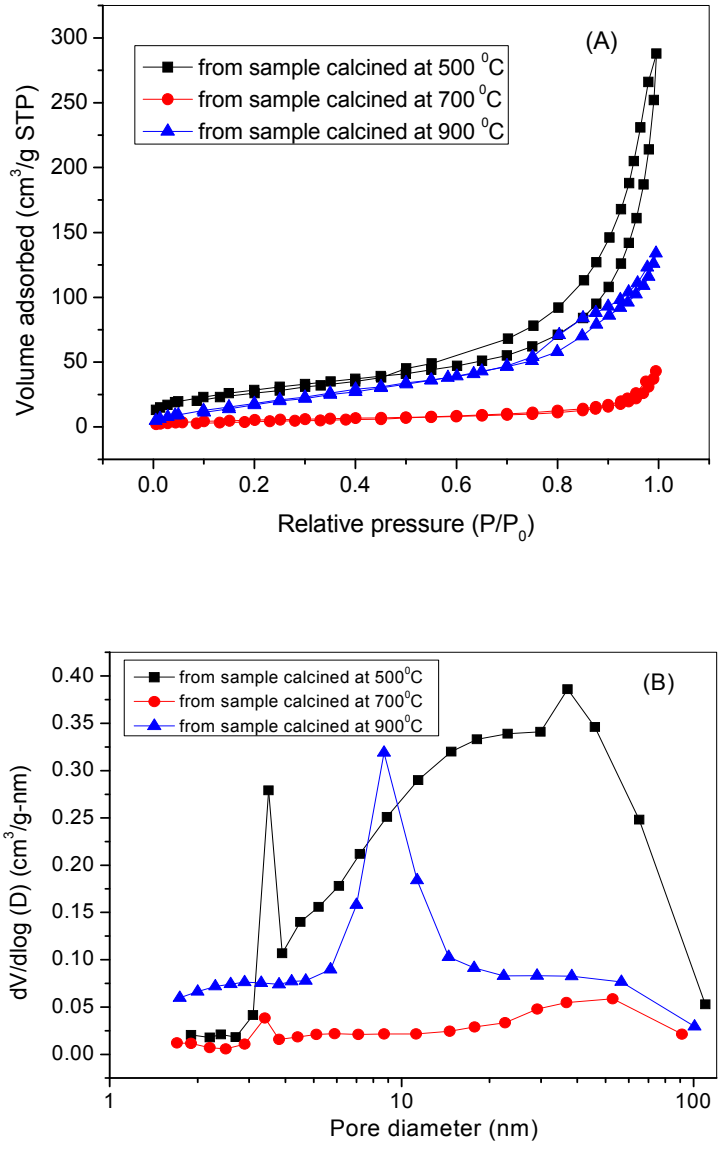

Figure S6 The nitrogen adsorption-desorption curves of the etched samples from particles calcined at 500℃, 700℃， 900℃ respectively

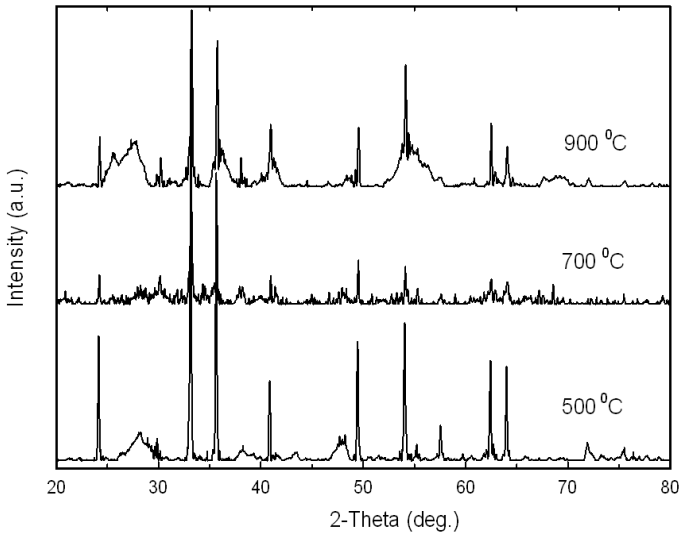

Figure S7 XRD patterns of the etched samples. The peaks at $2\theta = 24.16^{o}$, 33.20^{o}, 35.66^{o}, 40.90^{o}, 49.52^{o}, 54.12^{o}, 57.64^{o}, 69.62^{o} and 72.00^{o} respectively. According to the JCPDS card (33-0664), the particles contain crystallized hexagonal α-Fe_2O_3 and titania.

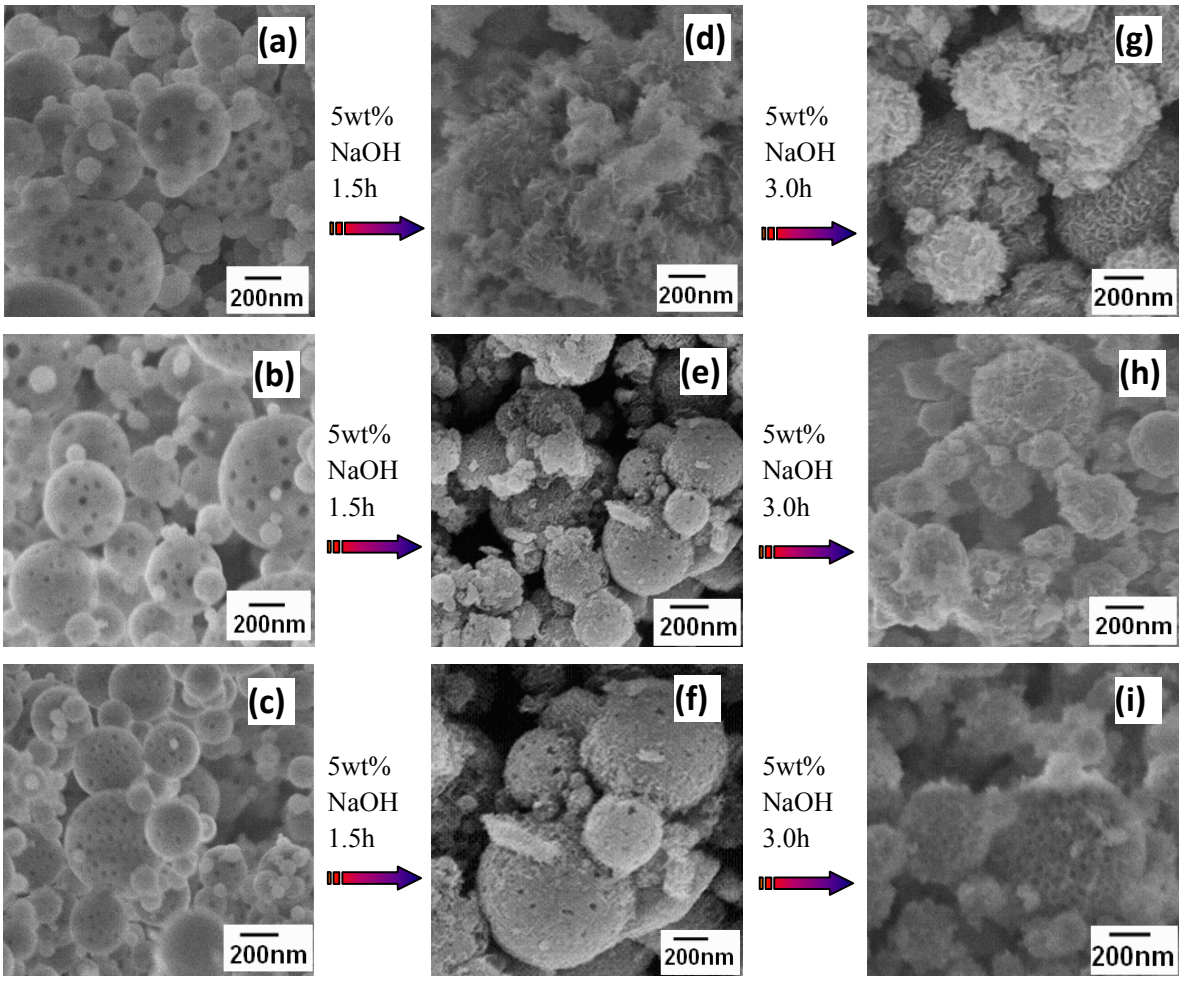

Figure S 8: Transition process of $TiO_2/SiO_2/Fe_2O_3$ spheres in 5wt% NaOH solution. (a) (b) (c) were precursor particles calcined at 500℃, 700℃,900℃ for 3h respectively; (d) (e) (f) and (g) (h) (i) the corresponding etched spheres which were treated 1.5h and 3.0h respectively in alkaline solution.

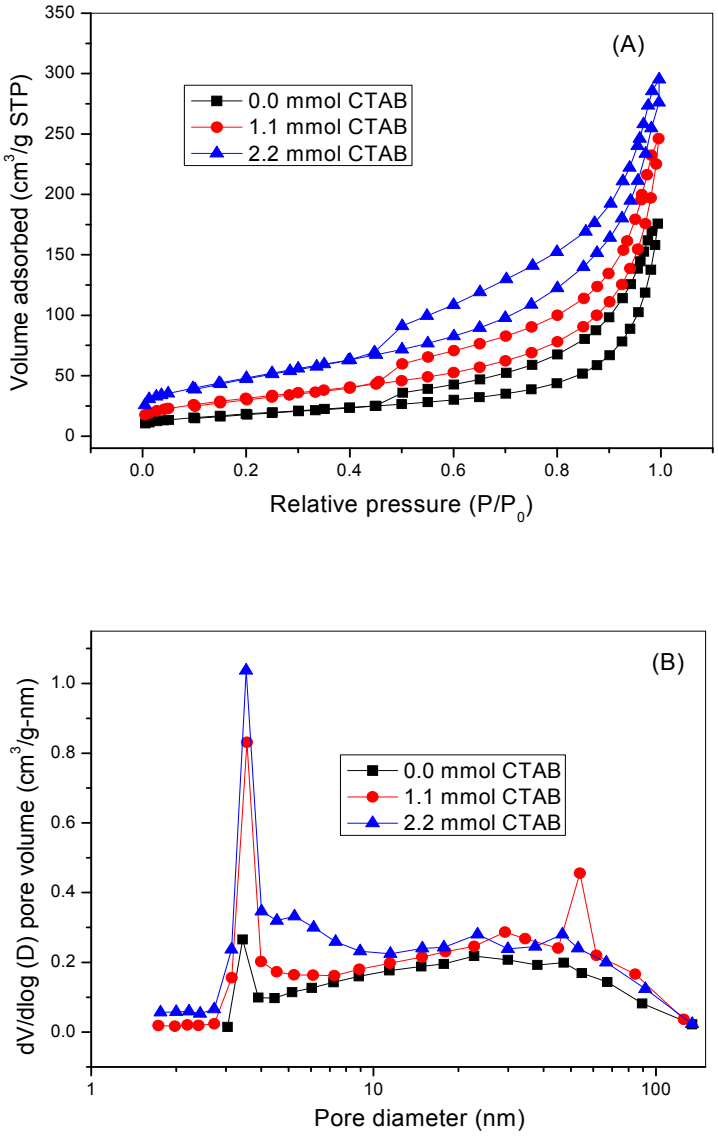

Figure S9: (A) the nitrogen adsorption-desorption curves and, (B) pore size distributions of the $SiO_2/TiO_2/Fe_2O_3$ precursor samples synthesized at different CTAB concentrations.

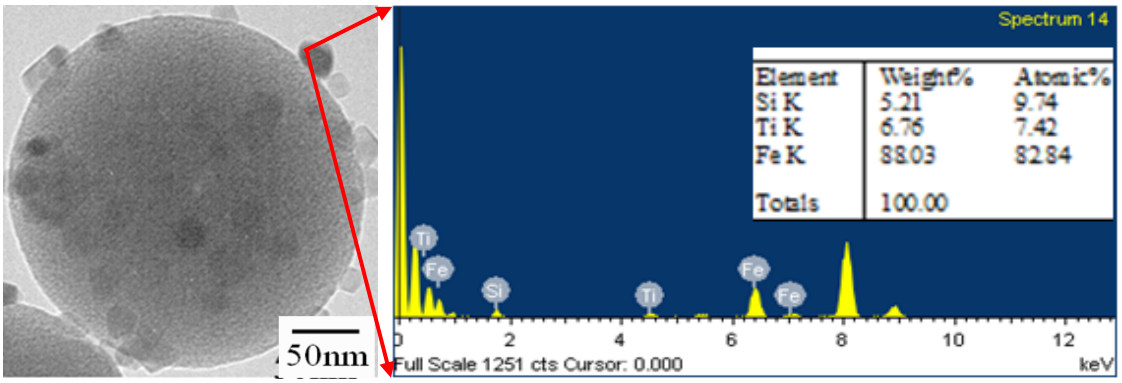

Figure S10 Composition of nanoparticles on the particle surface calcined at 500 ℃. Preparation conditions: 0.0 mmol CTAB, 3.6mmol $FeCl_3.6H_2O$.

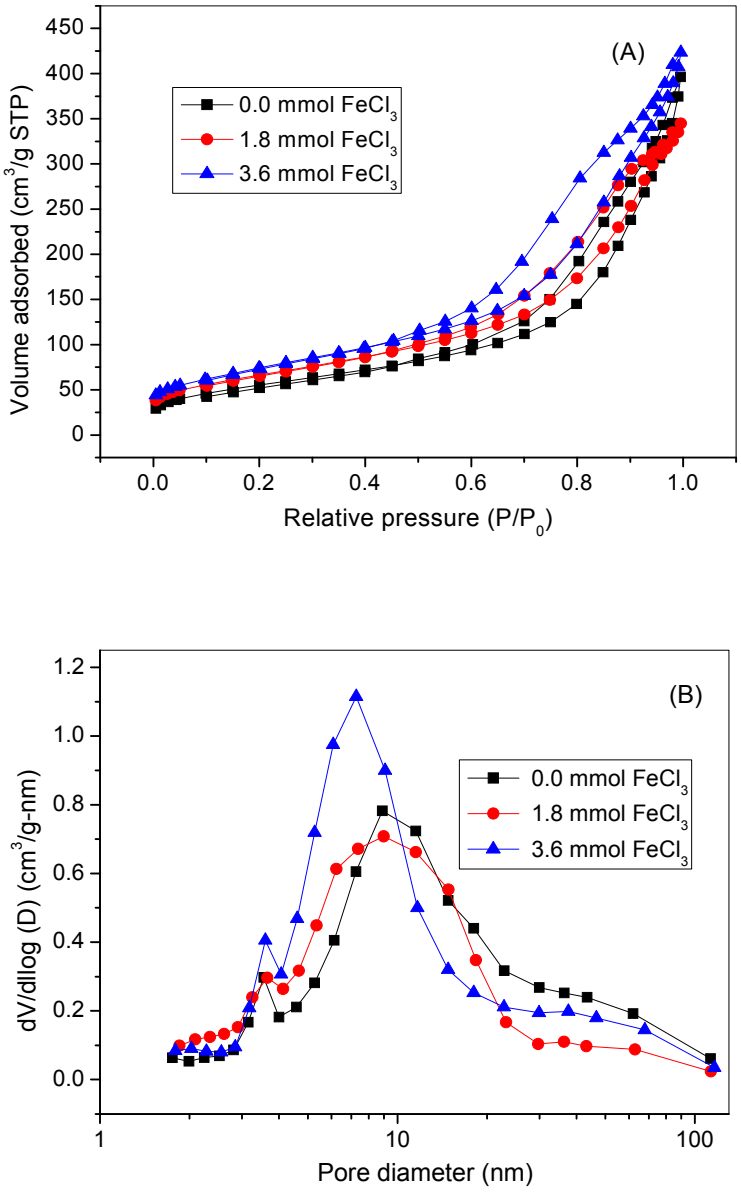

Figure S11: (A) the nitrogen adsorption-desorption curves and, (B) pore size distributions of the $SiO_2/TiO_2/Fe_2O_3$ precursor samples synthesized at different $FeCl_3$ concentrations.

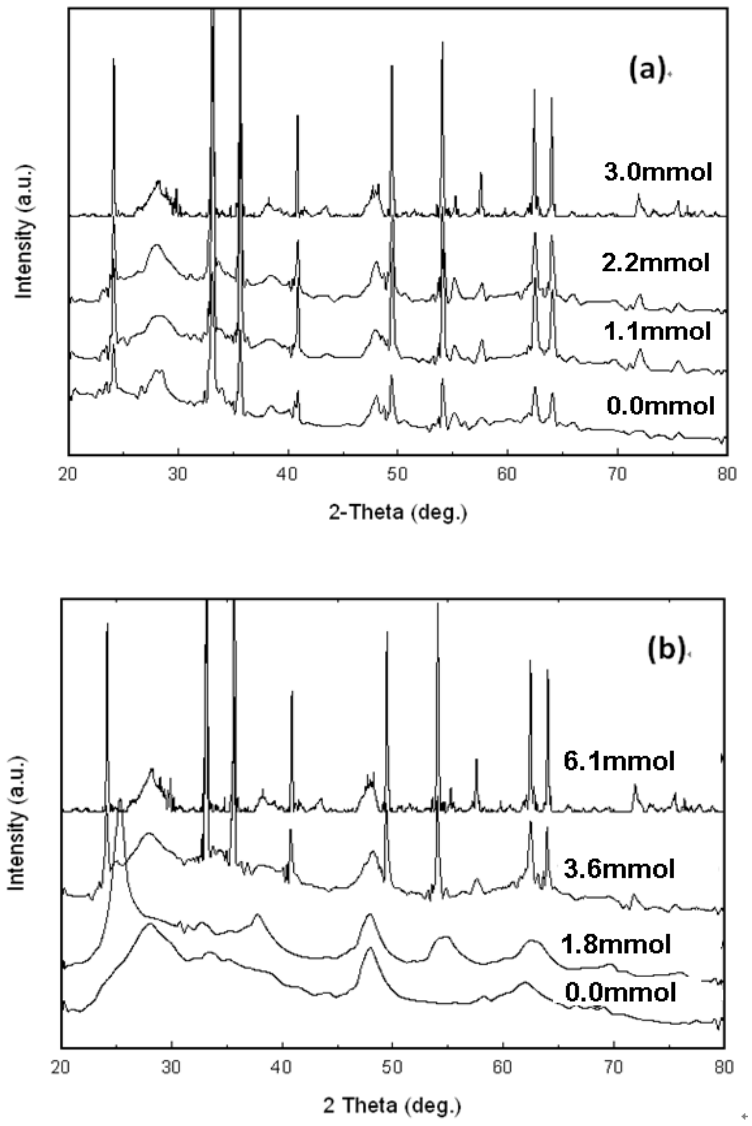

Figure S12 XRD spectra of the etched particles, (a) effect of CTAB content, (b) effect of $FeCl_3 \cdot 6H_2O$ content in the aerosol solution. All of the samples were a mixture of crystallized hexagonal α-Fe_2O_3 and titania (a). The increase of peak intensity of iron oxide with increasing loading of CTAB was due to the easier removal of silica from particles prepared at high CTAB content. For the second set of samples (b), rutile containing anatase titania was obtained without the presence of $FeCl_3 \cdot 6H_2O$, while pure anatase titania was prepared upon loading 1.8mmol $FeCl_3 \cdot 6H_2O$ in the aerosol solution. The crystal peaks were similar to the first set of etched sample when more than 3.6mmol $FeCl_3 \cdot 6H_2O$ was used. The result revealed that the amount of ferric colloids affected the type and growth of titania by impregnating its crystal lattice.

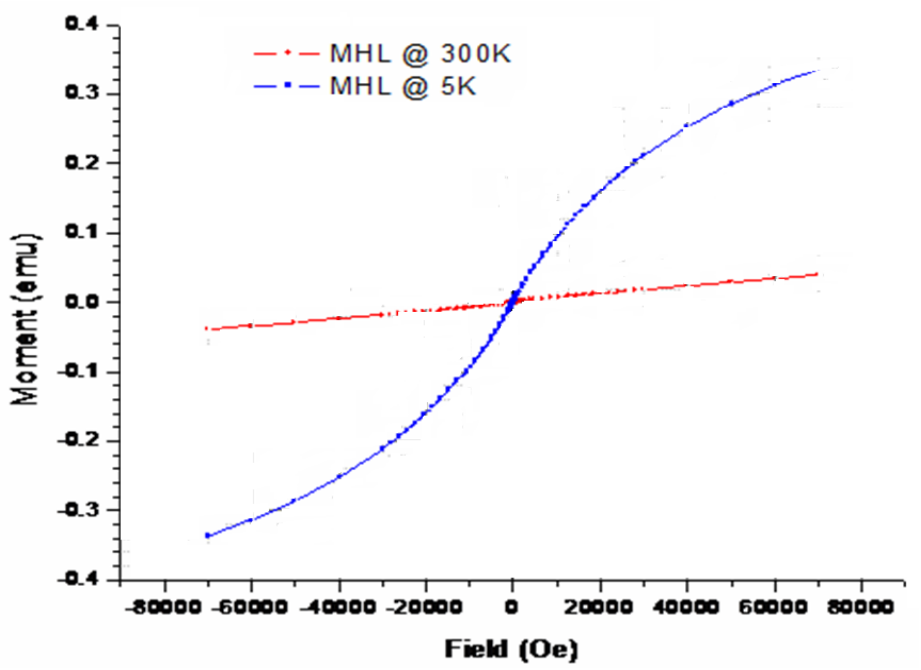

Figure S13 showed the magnetic-field dependence of magnetization for the etched particles. Liner dependence of magnetization on magnetic field and the absence of a magnetic hysteresis loop indicated that the etched spheres were paramagnetic in nature at room temperature (300K). In fact, the hollow particles were essentially super-paramagnetic possessing little hysteresis at low temperature (5K), suggesting minimal agglomeration of the magnetite nanoparticles.